Climate Change and Mountain Topographic Evolution in the Central Karakoram, Pakistan

Michael P. Bishop,* Andrew B. G. Bush,† Luke Copland,‡ Ulrich Kamp,§ Lewis A. Owen,# Yeong B. Seong,¶ and John F. Shroder, Jr.*

*Department of Geography and Geology, University of Nebraska–Omaha
†Department of Earth and Atmospheric Sciences, University of Alberta
‡Department of Geography, University of Ottawa
§Department of Geography, The University of Montana
#Department of Geology, University of Cincinnati
¶Department of Geography Education, Korea University

Mountain geodynamics represent highly scale-dependent interactions involving climate, tectonic, and surface processes. The central Karakoram in Pakistan exhibit strong climate–tectonic feedbacks, although the detailed tectonic and topographic responses to climate perturbations need to be systematically explored. This study focuses on understanding climate variations in relation to glacier erosion and relief production. Field data, climate modeling, remote sensing, geomorphometry, geochronology, glaciology, and geomorphological assessment are utilized to characterize climate change and geomorphic response. Climate simulations suggest that the region has experienced significant climate change due to radiative forcing over at least the past million years due to changes in Earth's orbital configuration, as well as more temporally rapid climate dynamics related to the El Niño Southern Oscillation. Paleoclimate simulations support geomorphological evidence of multiple glaciations and long-term glacier retreat. Mesoscale relief patterns clearly depict erosion zones that are spatially coincident with high peaks and rapid exhumation. These patterns depict extreme spatial and temporal variability of the influence of glacier erosion in the topographic evolution of the region. Results support the interpretation of high-magnitude glacial erosion as a significant denudational agent in the exhumation of the central Karakoram. Consequently, a strong linkage is seen to occur between global, or at least hemispheric, climate change and the topographic evolution of the Karakoram and the western Himalaya. *Key Words: central Karakoram, climate forcing, erosion, glaciation, landscape evolution.*

高山地球动力学代表与规模高度相关的，涉及气候，构造，和地面过程的相互作用。虽然还需要系统地探讨详细的构造和地形对气候扰动的响应，但是巴基斯坦中央喀喇昆仑已展现强有力的气候－构造反馈。本研究着重于了解有关气候变化与冰川侵蚀和生产救灾的相关性。利用现场数据，气候模型，遥感，地貌测量，年代学，冰川学，和地貌评估来表征气候变化和地貌反应。气候模拟表明，该地区在过去至少 100 年来，由于地球轨道构造变化的辐射力，已经经历了重大气候变化，以及与厄尔尼诺南方涛动有关的更快速的气候动态。古气候模拟支持多冰川和长期冰川退缩的地貌证据。中尺度救助格局图清楚地描绘了与高峰和险坡在空间上一致的侵蚀区。这些格局描述了在该地区的地形演化过程中冰川侵蚀影响的极端时空变异性。结果支持了高幅度冰川侵蚀是中央喀喇昆仑山峦一个重要剥离剂的解释。因此，能看到在全球，或者至少半球，气候变化和喀喇昆仑以及西部喜马拉雅地区的地形演变发展的密切联系。*关键词：中央喀喇昆仑山，气候强迫，侵蚀，冰川化，地貌演变。*

Las geodinámicas de montaña representan interacciones altamente dependientes de la escala en las que están involucrados procesos climáticos, tectónicos y topográficos. El Karakoram central de Pakistán muestra fuertes indicios de efectos climático–tectónicos, aunque las respuestas tectónicas y topográficas detalladas a las perturbaciones climáticas necesitan de una exploración sistemática. El presente estudio está enfocado a comprender las variaciones climáticas en relación con la erosión glaciar y la producción de relieve. Para caracterizar el cambio climático y la respuesta geomorfológica se utilizaron datos de campo, modelado climático, percepción remota, geomorfometría, geocronología, glaciología y análisis geomorfológico. Las simulaciones climáticas sugieren que la región ha experimentado cambio climático significativo por forzamiento radiativo durante por lo menos el pasado millón de años, causado por cambios en la configuración de la órbita terrestre, lo mismo que por la dinámica

Annals of the Association of American Geographers, 100(4) 2010, pp. 1–22
Initial submission, June 2009; revised submission, November 2009; final acceptance, January 2010
Published by Taylor & Francis, LLC.

climática de temporalidad más rápida asociada con la Oscilación Meridional de El Niño. Las simulaciones paleoclimáticas refrendan la evidencia geomorfológica de múltiples glaciaciones y recesión glaciar de larga duración. Los patrones de relieve a escala mediana claramente muestran zonas de erosión espacialmente coincidentes con picos altos y rápida exhumación. Estos patrones muestran variabilidad temporal y espacial extremas de la influencia de erosión glaciar en la evolución topográfica de la región. Los resultados apoyan la interpretación de erosión glacial de alta magnitud como agente de denudación significativo en la exhumación del Karakoram central. En consecuencia, se nota que existe un lazo fuerte entre el cambio climático global, o por lo menos hemisférico, y la evolución topográfica del Karakoram y el Himalaya occidental. *Palabras clave: Karakoram central, forzamiento climático, erosión, glaciación, evolución del paisaje*.

Mountain topographic evolution has been traditionally explained by collisional tectonics (Bender and Raza 1995; Turcotte and Schubert 2002). Molnar and England (1990) suggested that climatic forcing in the Quaternary enhanced glacial erosion in the Himalaya, thereby causing isostatic uplift of peaks and relief production. Conversely, Raymo, Ruddiman, and Froelich (1988) and Raymo and Ruddiman (1992) indicated that enhanced chemical weathering of exposed rock in the Himalaya could reduce atmospheric CO_2, such that tectonic forcing caused climatic cooling and glaciation. Central to these forcing arguments is the recognition of scale-dependent interactions among climatic, surface, and tectonic processes (Koons et al. 2002; Bishop, Shroder, and Colby 2003).

Key issues revolve around climate change, glacier erosion, erosion patterns, exhumation and uplift patterns, and relief production (Montgomery 1994; Finlayson, Montgomery, and Hallet 2002; Bishop, Shroder, and Colby 2003; Spotila et al. 2004; Whipple 2009). Complex feedback mechanisms are expected, although it is difficult to study these interactions because of the operational scale dependencies of numerous processes and polygenetic topographic evolution (Bishop et al. 2002; Bishop, Shroder, and Colby 2003). Consequently, many parameters and process rates need to be included, characterized, and quantified in the context of polygenetic topographic evolution. Issues and debate include the importance of isostatic uplift (Gilchrist, Summerfield, and Cockburn 1994), exhumation rates (Whittington 1996), climate control and erosion distribution and timing (Clift, Giosan, et al. 2008; Clift, Hodges et al. 2008; Rahaman et al. 2009), glaciers and relief production (Harbor and Warburton 1992; Hallet, Hunter, and Bogen 1996; Whipple and Tucker 1999; Whipple, Kirby, and Brocklehurst 1999), focused erosion and spatial coincidence (Zeitler, Koons et al. 2001; Zeitler, Meltzer, et al. 2001; Finlayson, Montgomery, and Hallet 2002; Finnegan et al. 2008), geomorphometry and erosion modeling (Montgomery and Brandon 2002; Bishop and Shroder 2004), and equilibrium concepts such as topographic steady state (Tomkin and Braun 2002). Finding definitive field evidence of strong impacts of climate change on mountain building has been difficult (Whipple 2009). Glaciation's role is probably significant (Whipple 2009), although numerous issues are unresolved because erosion-process mechanics are not fully understood, glacier erosion is not adequately accounted for in numerous studies, the timing and mechanisms of climate-controlled erosion in the Himalaya are controversial (Pelletier 2008; Rahaman et al. 2009; van der Beek et al. 2009), and demonstration of a cause-and-effect relationship between rapid exhumation and precipitation remains elusive (Pratt-Sitaula et al. 2009; Whipple 2009).

Nevertheless, there are three dominant conceptual models that attempt to characterize the nature of mountain geodynamics and relief production in active orogens. Researchers have recognized that variations in fluvial erosion are caused by precipitation gradients wherein rapid river incision causes larger scale mass movements that increase slope angles and relief (Burbank et al. 1996; Egholm et al. 2009). Associated rapid rock uplift produces threshold slopes where relief is governed by rock strength. The proximity of high-discharge rivers to massifs, with high exhumation and recently metamorphosed rocks, represents a new conceptual model termed a *tectonic aneurysm* (Zeitler, Koons et al. 2001; Zeitler, Meltzer et al. 2001), where tectonic and isostatic rock uplift beneath a focused erosion zone advects hot and weak material from the mid-crust toward the surface. Finally, the so-called glacial buzzsaw hypothesis suggests that the height of mountain ranges is primarily governed by glaciation and high-magnitude denudation, such that height and relief of mountain ranges are controlled by local climate rather than tectonic forces (Brozovic, Burbank, and Meigs 1997; Egholm et al. 2009).

The K2 mountain region in the central Karakoram in Pakistan represents an excellent natural laboratory for

studying these concepts of landscape evolution, the role of glaciers, and relief production. The central Karakoram contains some of the highest peaks in the world and exhibits extreme relief and high uplift rates (Foster, Gleadow, and Mortimer 1994; Seong et al. 2008). The evolution of the K2 mountain region has been dominated by glacial and meltwater stream systems (Seong et al. 2007; Seong, Bishop et al. 2009). This is unlike other massifs such as Nanga Parbat and Namche Barwa, which exhibit localized exhumation and are spatially coincident with large-discharge rivers (Zeitler, Koons et al. 2001; Zeitler, Meltzer et al. 2001; Finnegan et al. 2008). However, a paucity of information exists regarding long-term and high-altitude climate conditions, glacier fluctuations, and erosion and uplift patterns. Furthermore, the influence of glacier erosion on relief production is difficult to characterize, as glacier erosion includes numerous processes including a nonlinear interaction with the overall climate. In addition, complications involving the coupling of climate-modulated erosion with rock rheology and strength have been recognized (Schmidt and Montgomery 1995; Koons et al. 2002). Although point estimates of river incision and exhumation in the western Himalaya of Pakistan do exist (e.g., Foster, Gleadow, and Mortimer 1994; Burbank et al. 1996; Zeitler, Koons et al. 2001; Zeitler, Meltzer et al. 2001; Seong et al. 2008), little is known about climate forcing dynamics and erosion patterns within the K2 region.

The objectives of this article are to summarize our fieldwork studies on landscape dynamics in the central Karakoram during the summer of 2005. Specifically we undertake (1) an assessment of historical, modern, and future climate conditions and effects; (2) an assessment of the geomorphic conditions and the timing of glaciations; (3) characterization of relief and erosion patterns; and (4) characterization of modern glacial conditions to provide insight into the magnitude of glacier erosion and relief production.

Study Area

The central Karakoram occurs at the western end of the trans-Himalaya along the border between China and Pakistan (Figure 1). This active margin is partially the result of the Indian–Asian continental–continental collision at a rate of ~4.4 cm per year^{-1} (Minster and Jordan 1978). The central Karakoram is currently underthrust from the south by the Indian plate and from the north by the Asian plate, which has resulted in a crustal thickness of > 65 km (Molnar 1988; Searle et al. 1990; Searle 1991; Foster, Gleadow, and Mortimer 1994). The Indus River, one of the world's largest rivers, separates the central Karakoram from the Greater Himalaya. The region is bounded to the north by the Karakoram Fault and to the south by the Main Karakoram Thrust (MKT) that trends southeast across the region. Our study region (Figure 1) is composed of rocks of the Karakoram metamorphic series, Karakoram granitoids, Gasherbrum sedimentary deposits, Gasherbrum diorite, and the K2 and Muztagh Tower gneisses (Searle et al. 1990; Searle 1991).

Intense denudation in the central Karakoram is associated with rapid and spatially variable uplift rates that have unroofed Neogene gneiss domes (Mahéo et al. 2004; Seong et al. 2008). Foster, Gleadow, and Mortimer (1994) estimated denudation rates of 3 to 6 mm per year^{-1} during the last 3 to 5 Ma, with ≥6 km of exhumation at an altitude of 6,000 m above sea level (asl). The region exhibits extreme relief with valley floors averaging 2,000 m asl and more than seventy peaks that rise above 7,000 m asl, including K2 (8,611 m asl), Gasherbrum I (8,068 m asl), Broad Peak (8,047 asl.), and Gasherbrum II (8,035 m asl.). More than 80 percent of the landscape is at an elevation of between 3,000 and 6,000 m asl.

Climate

The climate dynamics of the region are dominated by the midlatitude westerlies and the southwest Asian summer monsoon, whereas microclimatic conditions vary significantly given topographic controls on precipitation and the surface-energy balance (Owen 1988; Hewitt 1989). Most of the precipitation occurs in the spring from the westerlies, although two thirds of the snowfall occurs during the winter and spring. Summer snowfall from the southwest Asian summer monsoon occurs (Hewitt 1989), although the westerlies likely also make summer contributions depending on the phase of El Niño Southern Oscillation (ENSO), which, during its warm phase, significantly reduces monsoon strength (e.g., Bush 2001). Measured weather data in the Karakoram are meager (Pant and Kumar 1997), although a climate station exists in Skardu, near K2 (Mayer et al. 2006), and the Pakistani government has installed high-altitude stations. In general, annual precipitation exhibits a large vertical gradient, with maximal amounts at Biafo Glacier from 4,900 m to 5,400 m (Wake 1989). On the southern slopes of K2, precipitation is about 150 mm to 200 mm per year^{-1} at 2,000 m to 3,200 m, 1,600

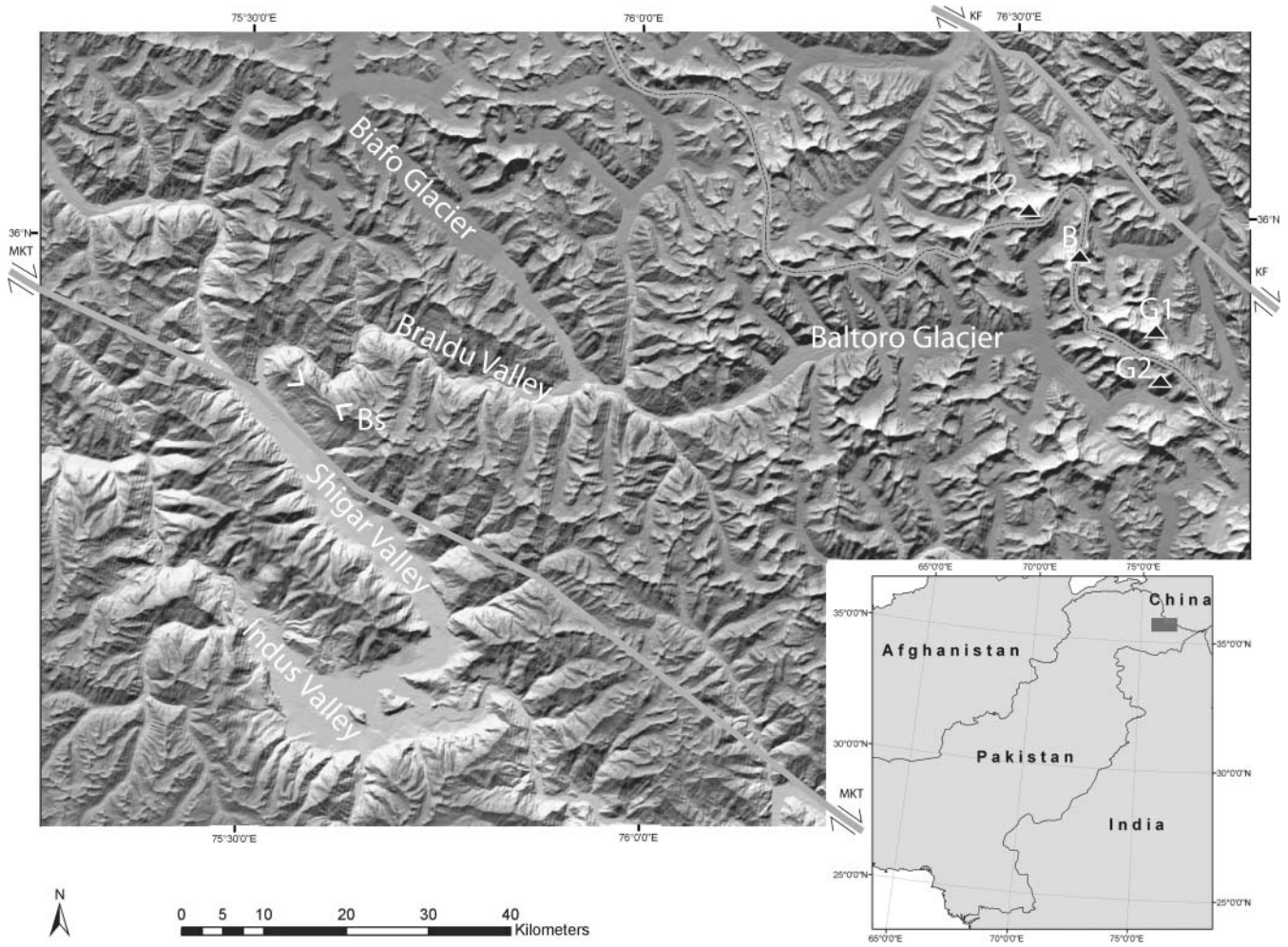

Figure 1. Shuttle Radar Topographic Mission shaded relief map of the K2 study region of the central Karakoram in northeastern Pakistan. Bs = Busper sackung; MKT = Main Karakoram Thrust; KF = Karakoram Fault; B = Broad peak; K2 = K2 peak; G1 = Gasherbrum 1 peak; G2 = Gasherbrum 2 peak.

mm per year^{-1} at 6,100 m, and about 2,500 mm per year^{-1} at 8,000 m (Mayer et al. 2006).

Surface Processes

The altitudinal zonation of the climatic-geomorphic conditions and their downslope relations have been previously recognized in terms of landforms and the sediment-transfer cascade (Hewitt 1989, 1993; Seong, Bishop et al. 2009). In this region, the process regimes alternate in concert with climate fluctuations. The overall sediment-transfer cascade involves glacier and fluvial incision, pervasive high frequency, moderate to high-magnitude mass movements onto and into glaciers and rivers, as well as catastrophic floods that remove valley fill out of the system (Shroder and Bishop 2000; Bishop et al. 2002).

The mass-movement types can be best considered in terms of regolith movement through common debris avalanches and flows, more deep-seated rock falls and rockslides, and massive sackung failures in which whole mountain ridges collapse internally along many interlinked and widely distributed shear planes. In all probability, debuttressing of rock slopes by glacier retreat during interglacials is likely to have produced many of the known rock falls and rockslides (Hewitt 1988, 1998a, 1999). In the Braldu River valley the huge Gomboro rockslide and the massive Busper sacking failure are seen to unroof the Neogene gneiss domes of Mahéo et al. (2004). Regional rates of erosion by mass-movement processes in the Himalaya are difficult to quantify, although their pervasive effects are obvious (Shroder 1998).

In the valley bottoms, fluvial and glacial processes are themselves the main erosional and transporting

agents. Hydrological monitoring of river discharges is extremely limited in the K2 region. Nevertheless, high summer discharges result from monsoon precipitation and summer melt regimes. Monsoonal flood peaks dominate rivers at lower elevations with 60 to 80 percent of discharge from rain, whereas 50 to 70 percent of total discharge at higher altitudes is glacier and snowmelt (Wohl 2000).

Drainage area is commonly used as a surrogate for discharge, but drainage area–discharge relations are far from linear because of the glacier-melt addition. For example, the Upper Hunza River drains ~5,000 km^2 of somewhat lower mountains and small glaciers north of the highest Karakoram chain. The discharge of the Upper Hunza is then doubled by its confluence with the short Batura River that drains the ~300 km^2 Batura Glacier (Gerrad 1990; Wohl 2000).

Stream-channel characteristics in the western Himalaya are characteristically diverse, with alternating reaches of exposed bedrock as well as long sections of gravel-armored beds. Coarse bedload has two opposing roles in bedrock erosion (Sklar and Dietrich 1998, 2001) such that at low sediment concentrations, an increase in gravel supply can provide more tools with which water can erode the bedrock, whereas at higher concentrations the channel bed can be protected. Rockfalls from unbuttressed walls during interglacials in the western Himalaya (Hewitt 1998a, 1999) can cause valley blocking and upstream sedimentation above the bedrock. Incision rates appear to be highest at intermediate levels of sediment supply and transport capacity. On channels steeper than about 20 percent, incision is probably dominated by episodic debris flows.

River incision into bedrock links topography to tectonics and climate but is poorly understood and is typically modeled using the so-called stream-power law (Howard 1980; Sklar and Dietrich 1998), which is appealing and has been used by many because it has a minimum number of parameters and can be empirically calibrated from topographic data. Nevertheless, it is not an actual physical law, is not directly process related, and must be applied with care (Hancock, Anderson, and Whipple 1998). In contrast, direct measures of incision rates based on terrestrial cosmogenic nuclide (TCN) surface exposure dating of strath terraces on the Indus and Braldu Rivers (Burbank et al. 1996; Seong et al. 2008), and other rivers in the Himalaya, might produce the most reliable data concerning incision rates. Along a 100-km reach, incision rates were found to vary from ~1 mm per $year^{-1}$ to 12 mm per $year^{-1}$, which is quite commensurate with inferred high uplift rates there (Zeitler 1985). Combined glacial and fluvial incision rates on Nanga Parbat appear even higher at ~22 ± 11 mm per $year^{-1}$ (Shroder and Bishop 2000) but are highly episodic and unlikely to be sustained over long periods. Nevertheless, highly focused river incision can affect crustal structure in mountain belts by changing the distribution of stress in the crust (Beaumont and Quinlan 1994; Wohl 2000; Koons et al. 2002). Rapid exhumation results from advecting crust, which is known as the tectonic aneurysm. This is considered the case at Nanga Parbat in Pakistan and Namche Barwa in Tibet (Zeitler, Koons et al. 2001; Zeitler, Meltzer et al. 2001; Finnegan et al. 2008).

Low-frequency, high-magnitude catastrophic floods in the western Himalaya and trans-Himalaya might be the single most important erosion process there because they scour the bedrock and transport such large quantities of sediment. Mass movement and glacial dams can be many hundreds of meters high, with the result that lakes impounded behind the barriers can become quite large. Eventually the impounded water will overtop most landslide barriers, or float most glacial ice, with the result that the large breakout floods can erode and transport considerable quantities of sediment (Cenderelli and Wohl 2003; Korup and Montgomery 2008). Imbricated flood boulders of up to 15 m in size serve as evidence of this process in the K2 region (Seong, Bishop et al. 2009).

Glaciers

The glaciers in this region over the last century were much larger than they are today (Mayewski and Jeschke 1979). Evidence of this is found in moraine deposits at high altitude, high-altitude erosion surfaces, and large U-shaped valleys that exhibit striated and ice-polished bedrock surfaces (Figure 2). Currently, there are more than thirty glaciers over 20 km in length in the central Karakoram. The glaciers in this region, including the Batura, Hispar, Biafo, and Baltoro Glaciers, comprise some of the longest midlatitude ice masses in the world. The surface gradients of the glaciers range from very steep to gentle, with the largest glaciers often having ablation areas with very low surface slope angles (e.g., Baltoro Glacier has an average surface slope angle of about 2 degrees over its lowermost 35 km). Supraglacial debris covers most glaciers in their ablation zone. The thickness of this supraglacial debris is highly variable, although there is a general increase down-glacier, with maximum depths greater than 5 m.

Figure 2. Ice-polished bedrock surfaces on the south side of the Braldu Valley.

Thick debris effectively insulates (Hagg et al. 2008), thereby reducing ablation rates and allowing glaciers to exist at lower altitudes. Most of the glaciers are of winter accumulation type, reflecting the dominant influence of the midlatitude westerlies, although significant monsoon-related summer snowfall does occur. Snow and ice avalanching is significant given the extreme relief and feeds many glaciers. Ice velocities have been documented to increase by up to double in the summer compared to the winter due to increased meltwater (Copland et al. 2009; Quincey et al. 2009), and many glaciers actively incise the landscape (Figure 3).

The Karakoram is known for its many surging glaciers, and new data indicate an increase in the number of surging and advancing glaciers (Hewitt 1969, 1998b, 2005, 2007; Copland et al. 2009). Glaciers in this region are thought to be more responsive to change in precipitation than in temperature (Derbyshire 1981; Shi 2002; Owen et al. 2005), although systematic ablation studies are limited to short-term measurements

Figure 3. Urdukas West Glacier is a tributary glacier of the Baltoro Glacier system on the south side of the valley. The glacier has vertically incised into the landscape generating steep valley slopes and extreme relief. The width of the glacier is approximately 261 m.

such as Mihalcea et al. (2006). Unfortunately, individual glacier and regional mass balance trends are not currently known with any certainty.

Climate Modeling

To better understand climate variations, we conducted seventy-year simulations with a fully coupled atmosphere–ocean general circulation model (see Bush and Philander [1999] for details on the model configuration). Specifically, we examine paleoclimate conditions for the Last Glacial Maximum (LGM ~21 ka), 16 ka, 9 ka, and 6 ka, and compared results to modern climate conditions. We also simulated a future climate scenario assuming CO_2 forcing double that of the present day. Insolation data in all simulations are from Berger (1992) and ice-sheet topography is from Peltier (1994). The atmospheric model is spectral and has an equivalent spatial resolution of ~2.250 of latitude by 3.750 of longitude. The ocean model has comparable resolution.

Topographic heights are included in the model by spectrally decomposing digital elevation data and then truncating the resulting wave-number expansion at the smallest wave-number resolved by the model (wave-number thirty using a rhomboidal truncation scheme). Any resulting Gibbs oscillations are damped by a spectral smoothing technique (Navarra, Stern, and Miyakoda 1994). Although the model resolution is relatively fine from a global perspective, it is quite coarse when examining results on spatial scales of hundreds of kilometers. For this reason, spatial averages over multiple grid cells are commonly used to describe regional climate fluctuations because the averaging procedure produces statistically more significant and robust results. Nevertheless, the global model is incapable of generating detailed results on spatial scales smaller than a few hundred kilometers, and alternative methods such as statistical downscaling (e.g., Easterling 1999; von Storch and Navarra 1999; Schoof and Pryor 2001) or nested modeling methodologies (e.g., Christensen et al. 2001; Raisanen, Rummukainen, and Ullerstig 2001) are required to produce climate data in such fine spatial detail. We specifically focus on temperature and snow accumulation, as these parameters are most significant in governing glacier fluctuations and erosion.

Our numerical simulations reveal a monotonic decrease in the amount of snow accumulation averaged over the Himalayan area of 60–105°E, 24–44°N from the LGM to today, and this trend continues most dramatically in a doubled CO_2 climate (Figure 4). Simulated snow cover over the study region in the central Karakoram, averaged over 70–80°E, 30–37°N, indicates similar trends. As the atmosphere warms from a glacial to interglacial state (and beyond), the amount of snow accumulation in the western Himalaya decreases.

The spatial pattern of difference in snow accumulation indicates large changes along the front range of the Himalaya (Figure 5). From the LGM to 6 ka, snow accumulation was higher than today along the entire length of the front range that faces the influence of the summer monsoon and its orographic precipitation. The accumulation along the southwestern front of the Himalaya was highest, however, in the 16 ka simulation despite the fact that orbital obliquity, and hence monsoon strength, did not reach its maximum until 11 ka. Dramatic decreases in snow accumulation in the doubled CO_2 simulation occur across the entire study region. Our numerical simulation results indicate that the area around and to the south of Nanga Parbat has been in the past more susceptible to change than the central Karakoram (Figure 5B–E). In a doubled CO_2 climate, however, both regions are affected to a similar degree in terms of reduced snow accumulation (Figure 5F).

Summertime radiative forcing in the region increases between the LGM and 11 ka due to the increase in Earth's angle of obliquity. This strengthens the summertime monsoon and should, given the increase in temperature, increase precipitation during the summer months. The decline in snowfall is indicative of a change in type of precipitation, with more rainfall occurring rather than snowfall in a warmer climate.

Interannual variability associated with ENSO is also a major factor regulating precipitation in this region. As best as can be determined, during the LGM, ENSO was frequent but of small amplitude (Bush 2007) and would likely not have had as much influence on the summertime monsoon as it does today. The competition between monsoon southwesterly winds and the midlatitude westerlies that flow over Europe and the Caspian Sea is a delicate balance that determines the type of precipitation in this study region. If the monsoon is weak, the midlatitude westerlies are able to penetrate further east, bringing colder winds and more snowfall to the region. If the monsoon is strong, however, then warm, moist air dominates the region and snowfall is reduced but rainfall is enhanced.

Compared with the climate through the last glacial cycle, the most dramatic change simulated is the one between today and that of a climate with doubled atmospheric CO_2. For the study region, the simulated change between today and a possible future climate is

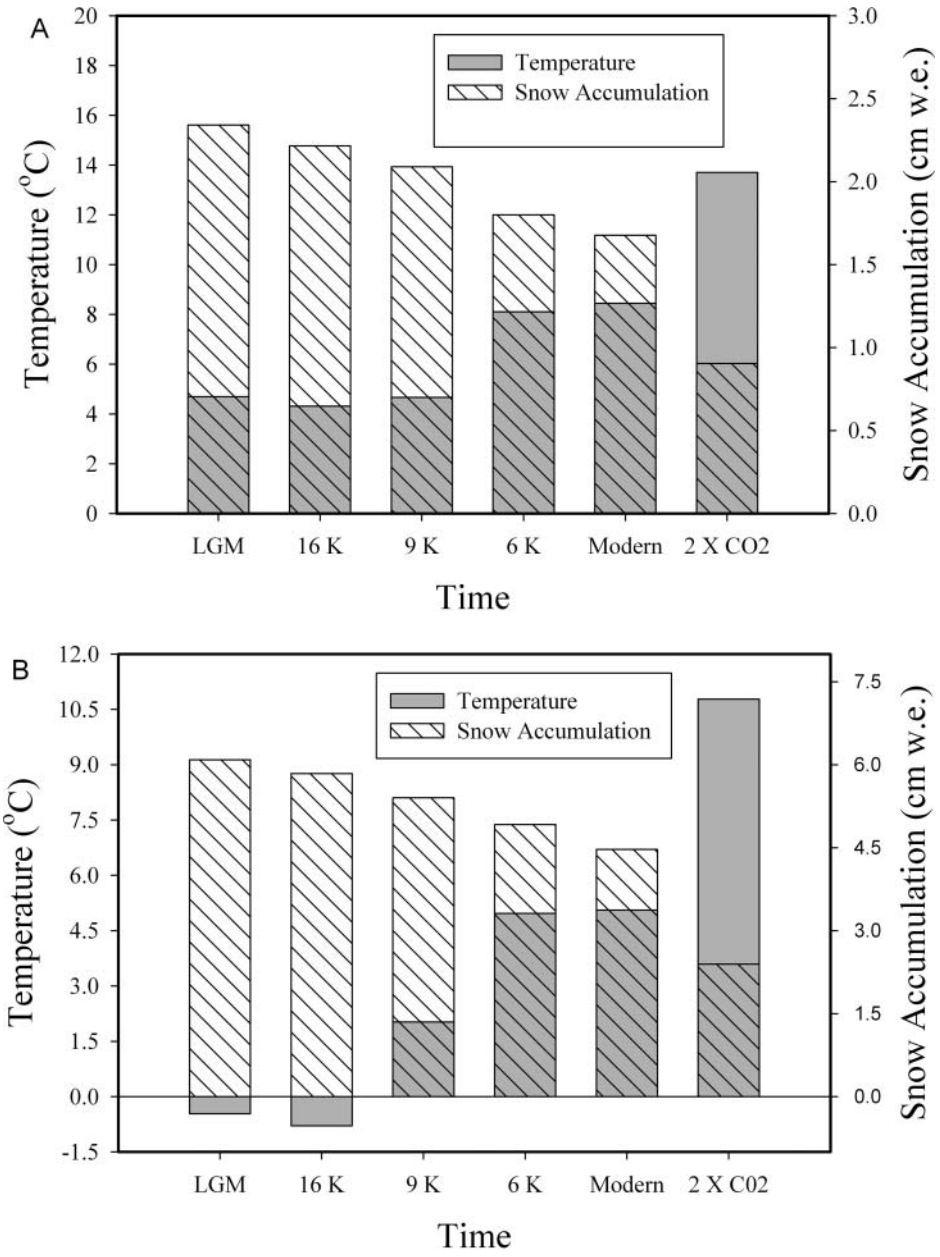

Figure 4. Annual mean temperature and snow accumulation averaged over (A) 60–105°E, 24–44°N; (B) 70–80°E, 30–37°N.

greater than the change between today and the LGM. This reflects the fact that a doubling of atmospheric CO_2 places our climate outside the bounds of the naturally varying glacial and interglacial climates of the Late Quaternary. Implications for future glacial mass balance and freshwater resources for the countries in this region are profound.

Timing and Style of Quaternary Glaciation

We examined the Quaternary glacial history of the central Karakoram using geomorphic mapping of landforms and sediments and ^{10}Be TCN surface exposure dating of boulders on moraines and glacially eroded surfaces (Seong et al. 2007). We mapped landforms (strath terraces, flood deposits, and landslides) and assessed ^{10}Be TCN ages to better understand glaciations and landscape evolution (Seong et al. 2008; Seong, Bishop et al. 2009). Details of our methods related to sampling and laboratory analysis for ^{10}Be TCN dating are provided in Seong et al. (2007, 2008; Seong, Bishop et al. 2009).

We recognized four glacial stages in the Skardu Basin and the Shigar and Braldu Valleys of the central Karakoram, which were defined as Bunthang glacial stage (>0.7 Ma), Skardu glacial stage (Marine Oxygen

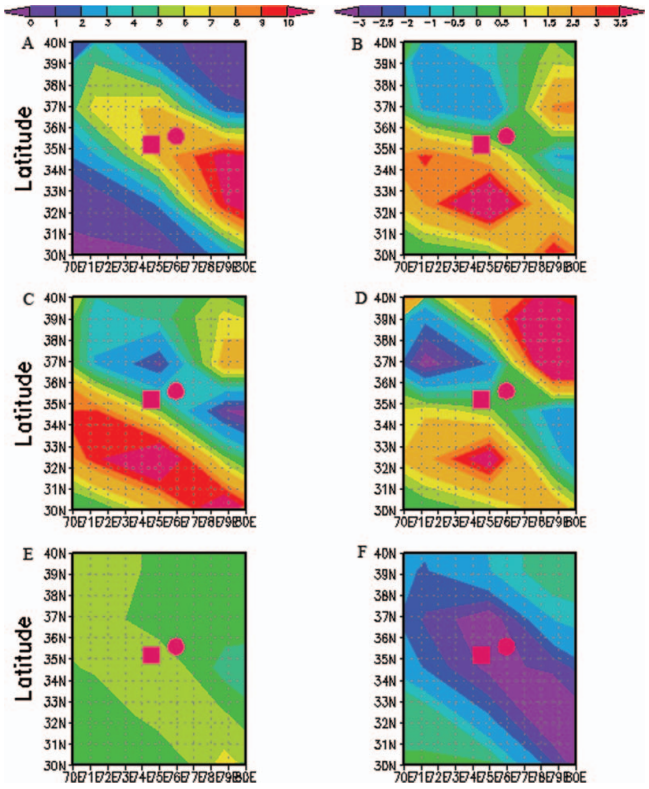

Figure 5. Annual mean snow accumulation (cm w.e.) over 73–80E, 32–37N. K2 is depicted by a red circle and Nanga Parbat is represented by a red square. (A) Modern climate simulation (control), with color scale range depicted overtop. (B–F) Last glacial maximum, 16 ka, 9 ka, 6 ka, and 2× CO_2, respectively, with color scale range depicted over B.

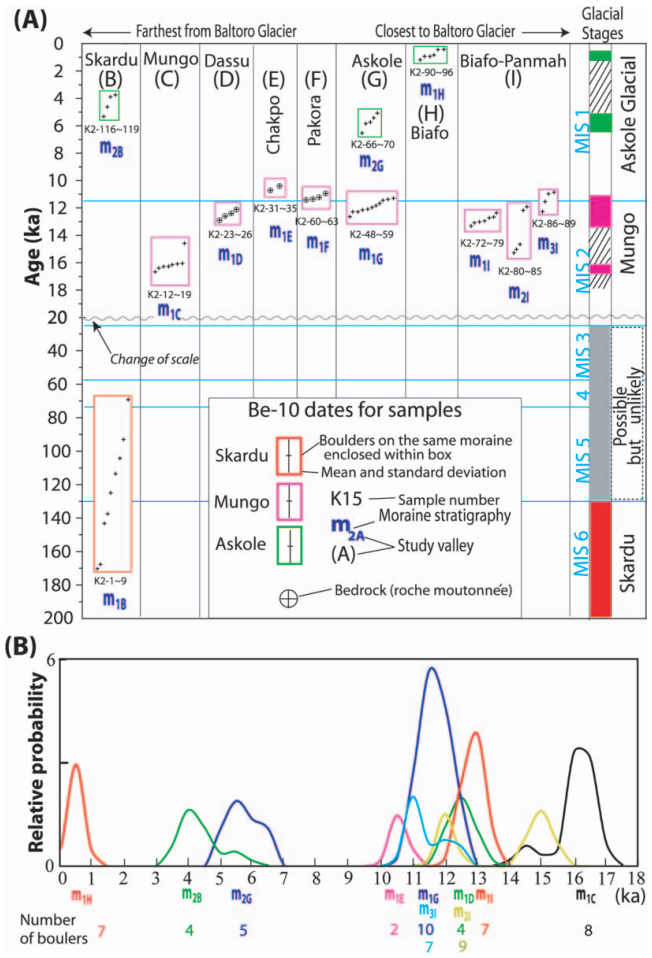

Figure 6. ^{10}Be TCN surface exposure ages for boulders on the moraines dated in the central Karakoram (from Seong et al. 2007). (A) Scatter plots of ages on each moraine. Each box encloses one landform. Marine oxygen isotope stages (MIS; after Martinson et al. 1987) are shown in light blue. The vertical scale changes from 20 ka and its boundary is marked by a light gray undulating line. (B) Probability distributions for ^{10}Be TCN surface exposure ages of each glacial advance after 18 ka. Each different color represents a landform formed during a different glacial stage.

Isotope Stage [MIS] 6 or older); Mungo glacial stage (MIS 2); and Askole glacial stage (Holocene). The glacial geologic evidence shows that glaciers oscillated several times during each glacial stage. Glacial advances during the oldest stage, the Bunthang, were not well defined because of the lack of preservation of landforms and sediments. In contrast, the glacial geologic evidence for the Mungo and Askole stages is abundant throughout the study region and we were able to define glacial advances that likely occurred at ~16, ~11–13, ~5, and ~ 0.8 ka (Figure 6). Furthermore, our data show that the extent of each progressive glaciation throughout the region became increasingly more restricted over time (Seong et al. 2007; Seong, Bishop et al. 2009). In the Braldu and Shigar valleys, glaciers advanced more than 150 km during the Bunthang and Skardu glacial stages, and glaciers advanced more than 80 km beyond their present positions during the Mungo glacial stage. In contrast, during the Askole glacial stage, glaciers only advanced a few kilometers from present ice margins. We calculated the equilibrium-line depression for the Mungo glacial stage to be ~500 m (Seong, Bishop et al. 2009).

Seong et al. (2007) argued that glaciers in the central Karakoram likely responded to the same forcing that caused changes in Northern Hemisphere oceans and ice sheets. These changes are likely teleconnected via the midlatitude westerlies and also to changes in monsoon intensity. Owen et al. (2008) highlighted the fact that the extent of glaciation between adjacent regions within the Himalayan–Tibetan orogen can vary considerably. This is particularly well illustrated across northern Pakistan and northern India for the Late Glacial at about 14 to 16 ka, coincident with the Mungo glacial stage of northern Pakistan. During this time in the

central Karakoram an extensive valley glacier system extended more than 80 km from the present ice margin, whereas in the Hunza valley to the northeast and Muztag Ata-Kongur Shan to the north, for example, glaciers only advanced a few kilometers from their present position (Owen et al. 2002; Seong et al. 2007; Owen et al. 2008; Seong, Owen et al. 2009). In Ladakh, to the southeast of these regions, there is little evidence of a glacier advance at this time, and when glaciers did advance they were restricted to a few kilometers from their present ice margins (Owen et al. 2006; Owen et al. 2008). Furthermore, to the south of Ladakh, in the Lahul Himalaya, glaciers advanced more than 100 km beyond their present positions at this time (Owen et al. 2001; Owen et al. 2008). These contrasts in the extent of glaciation within a relatively small region of the Himalaya and trans-Himalaya highlight the important local climatic gradients and the strong topographic controls on climate forcing and glaciation.

Nevertheless, by recalculating all of the TCN ages for moraine boulders and glacially eroded surfaces throughout the Himalayan–Tibetan region, Owen et al. (2008) were able to make broad statements regarding the synchroneity of glaciation. In essence, glaciers throughout monsoon-influenced Tibet and the Himalaya and the trans-Himalaya (including the central Karakoram) appear to have responded in a similar fashion to changes in monsoon-driven and Northern Hemisphere cooling cycles alone. In contrast, glaciers in the far western regions of the Himalayan–Tibetan orogen are asynchronous with the other regions and appear to be dominantly controlled by the Northern Hemisphere cooling cycles and by the influential interaction between the relative strengths of the westerlies and the summer monsoon.

Geomorphometry

Such dramatic glacier fluctuations generate extreme relief and U-shaped valleys. Relief, however, might not always be related linearly to erosion and erosional efficiency. For glacier erosion, research has indicated that glaciation can limit relief up to some altitude approaching the equilibrium-line altitude (ELA) and that erosion fluctuations at the ELA can generate extreme relief (Brozovic, Burbank, and Meigs 1997; Bishop, Shroder, and Colby 2003). Given the anisotropic nature of relief, as a function of a variety of surface processes and deformation, it is necessary to quantitatively characterize the topography and compare high-relief regions, as the topography inherently represents the interplay among climate, tectonics, and surface processes (Wobus et al. 2006).

We conducted an analysis of the topography over the western Himalaya of Pakistan using Shuttle Radar Topographic Mission (SRTM30) data, acquired from the Spaceborne Imaging Radar-C. The SRTM30 data were constructed at thirty arc-second spacing, similar to GTOP030 data. GTOP030 data points were used where SRTM data were invalid (i.e., radar shadows). We projected the data set (Universal Transverse Mercator) and resampled (bilinear interpolation) it to generate an SRTM30 data set with a grid resolution of 1 km. Given the coarse resolution of the data set, altitude estimates and slope angle magnitudes are generalized and underestimated. The projected SRTM30 data set, however, adequately characterizes the relief structure of the landscape and permits a first-order assessment of the topography.

Geomorphometric analysis consisted of analyzing and comparing topographic regions (14,400 km^2) that were centered on high-altitude peaks including Batura Mustagh, Distaghil, K2, Nanga Parbat, and Rakaposhi (Figure 7A). Hypsometric analyses permitted an examination of the altitude/area relationship and the relative amount of mass removed from each region. It is important to note that the relative patterns of hypsometric curves are generally related to erosion potential, although the hypsometric integral does not represent an absolute magnitude of erosion given systematic and nonsystematic biases in the digital elevation model (DEM).

Scale-dependent analysis of the topography was used to characterize the relief structure of each region. Specifically, we performed semivariogram analysis and compared every grid cell to every other grid cell within each region. Within an $n_x \times n_y$ grid there will be N point pairs, where $N = n_x^2\ (n_y^2 - 1)/2$. The variance component is $\Delta z = (z_1 - z_2)^2$, and the horizontal distance is $\Delta x = [(x_1 - x_2)^2 + (y_1 - y_2)^2]^{0.5}$. The variance was summed over a binned horizontal distance interval (1 km).

We also conducted spatial analysis to assess the degree of landscape concavity and convexity. The approach represents a hemispherical analysis of the topography to measure the angular relation between the surface relief and the multidirectional horizontal distances. Yokoyama, Shirasawa, and Pike (2002) referred to this measure as *openness* and provided a quantitative description of positive openness (P) and negative openness (N). We computed P and N images using a radius distance of 30 km around each grid cell

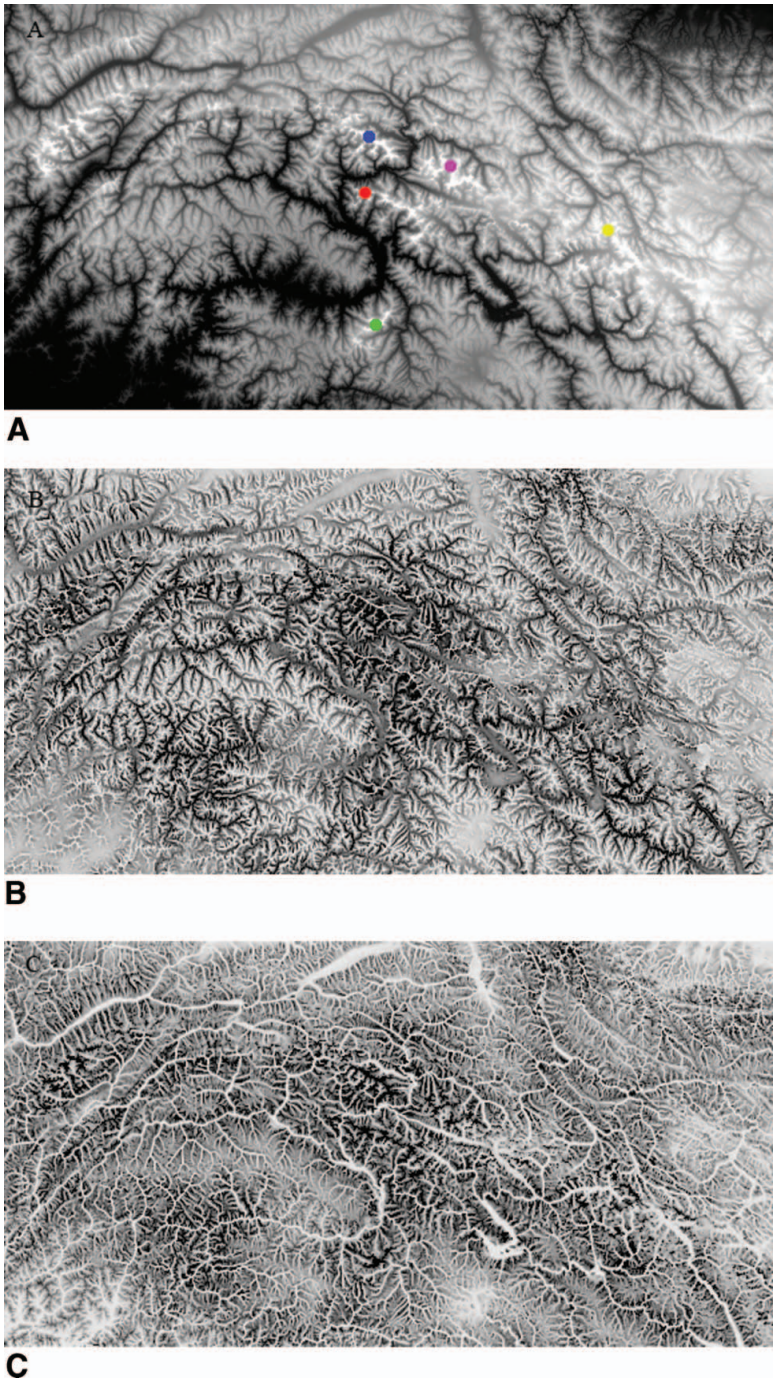

Figure 7. Subsection of the Shuttle Radar Topographic Mission (SRTM30) data set that was used for geomorphometric analysis. (A) Geomorphometric analysis of 120 × 120 km regions included Nanga Parbat (green dot), Rakaposhi (red dot), Batura (blue dot), Distaghil (magenta dot), and K2 (yellow dot). (B) Positive-openness measure. Dark gray tones represent concavity, and lighter gray tones depict convexity. (C) Negative-openness measure. Light gray tones represent concavity, and darker gray tones represent convexity.

(Figure 7B, C). We wanted to investigate the potential of landscape convexity and concavity to be used for assessing spatial variations in relief.

Hypsometric analysis revealed that the majority of the K2 massif (88 percent) occurs between 4,000 and 6,000 m asl, with an estimated mean elevation of 5,064 m asl. Average altitudes for the Nanga Parbat (3,598 m asl), Rakaposhi (3,895 m asl), and Distaghil (4,609 m asl) regions depict a systematic north and easterly increase in average altitude toward K2.

The hypsometric curve for the K2 region is similar in shape to Nanga Parbat's depicting similar relief at high altitudes due to deep glacier erosion, although less pervasive river incision at lower altitudes accounts for more mass there at K2 (Figure 8). In contrast, the Rakaposhi curve reveals more high-altitude land mass and a

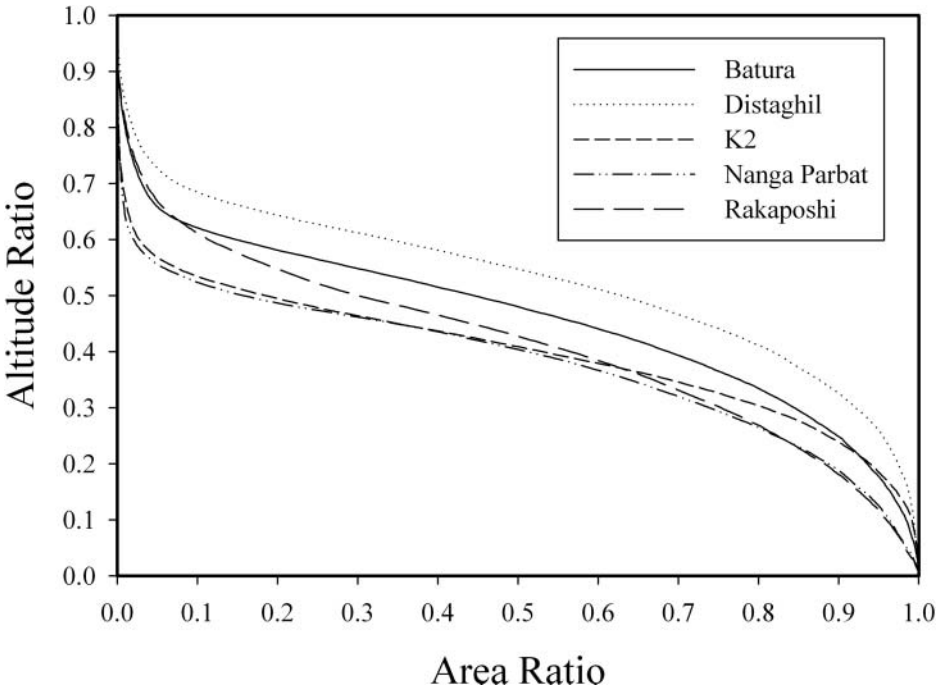

Figure 8. Hypsometry of the Batura, Nanga Parbat, Rakaposhi, Distaghil, and K2 regions. Each region was centered on each peak and represents 14,400 km^2.

similar low-altitude mass distribution, whereas the Distaghil region exhibits relatively more land mass at all altitudes. This indicates a difference in the surface processes responsible for erosion at various altitudes and the degree to which incision and hillslope processes dominate mass removal.

These results can be viewed from a denudational unloading perspective by comparing the hypsometric integrals (HI). Nanga Parbat exhibited the lowest HI (0.3789). Going north, Rakaposhi and Batura are characterized by HI values of 0.4125 and 0.4586. To the west of K2, Distaghil exhibits a value of 0.5268, and the K2 value is 0.3986. This suggests that denudational unloading is greatest at Nanga Parbat and K2, compared to the Hunza region of the Karakoram. In addition, these two regions exhibit the hypsometric signature of the glacial buzzsaw model. Given the relative high mean altitude of the K2 region and relatively large glaciers, we might expect K2 to exhibit the lowest integral value, although the removal of glaciers with respect to DEM altitude values would produce a lower value.

Assuming that greater relief is related to the magnitude of erosion, our variogram analysis reveals a different pattern. The Rakaposhi region exhibits the greatest relief at all lag distances (Figure 9). This is consistent with the coupled river-incision and slope-failure model. At lag distances $\leq$18 km, the Distaghil region exhibits greater mean relief than Nanga Parbat, but Nanga Parbat exhibits greater relief at lag distances $\geq$18 km. The relatively high mean relief characterizes the influence of the size of the fluvial drainage network. K2 exhibits the least amount of relief at all lag distances and the relief signature is best explained by the glacial buzzsaw model.

Analysis of the concavity and convexity patterns in the topography of the western Himalaya provides insight into the nature of erosion. The positive-openness measure uses the minimum zenith angle to characterize concavity and convexity (Figure 7B). The magnitude of the concavity is related to the mesoscale relief. The spatial patterns of concavity clearly show regions of relief where erosion has removed more lithospheric mass. Spatially contiguous concavity zones include Nanga Parbat and the Hunza region (Rakaposhi, Batura, Distaghil). These patterns explain the increased scale-dependent relief at Nanga Parbat, Rakaposhi, Batura, and Distaghil. K2 does exhibit significant mesoscale relief immediately surrounding the mountain, although it exhibits less of a spatial predominance of extreme relief compared to the aforementioned regions. Furthermore, areas of low relief include the Kohistan region to the west of Nanga Parbat and the Deosai plateau to the east of Nanga Parbat.

The negative-openness measure of concavity and convexity provides additional insight into the nature of erosion (Figure 7C). This measure uses the maximum zenith angle to characterize concavity and convexity.

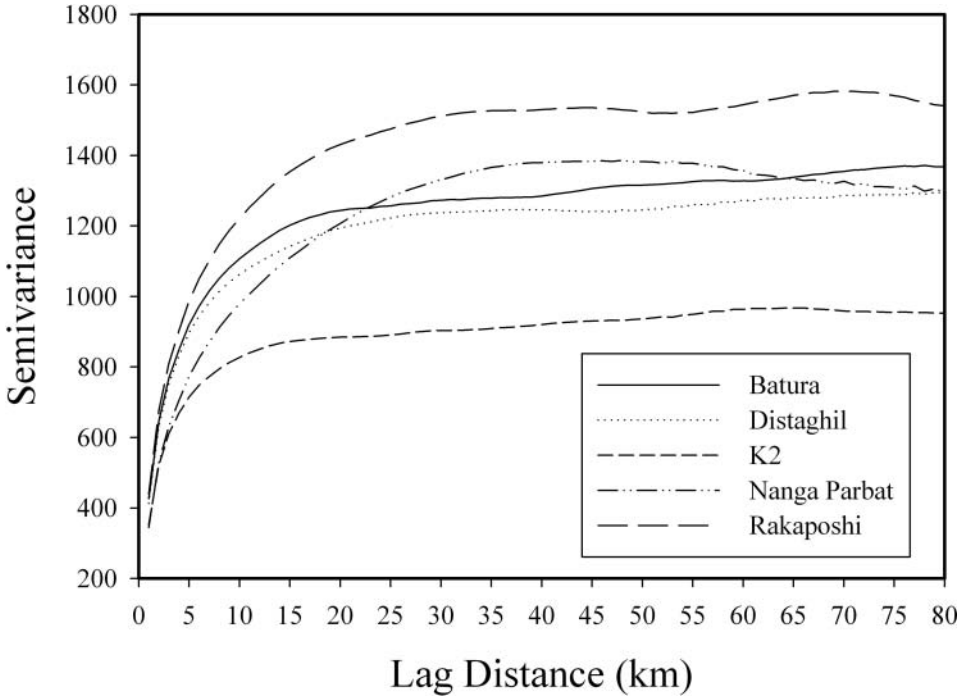

Figure 9. Semivariograms for the Batura, Nanga Parbat, Rakaposhi, Distaghil, and K2 regions of the central Karakoram.

The spatial patterns and magnitude of concavity identify the influence of river incision and the drainage network on the landscape. For example, the relatively high-magnitude concavity identified the rapid river incision associated with the Indus and Astor Rivers near Nanga Parbat, where rapid uplift is known to occur (Zeitler, Koons et al. 2001; Zeitler, Meltzer et al. 2001). Collectively, these results demonstrate the polygenetic nature of erosion and relief production, as a particular landscape will exhibit multiple geomorphometric signatures that characterize different landscape evolution models.

Glaciological Observations

Glaciological measurements in the K2 region of the central Karakoram in summer 2005 focused along a ~50 km length of Godwin Austen and Baltoro Glaciers below K2, as well as the nearby Biafo Glacier. To date even basic information such as ice depths and surface velocities are poorly known for these ice masses, yet this information is crucial for understanding glacier response to climate change and the role of glacier erosion in landscape evolution.

Surface Velocities

We made surface velocity measurements from the repeated positioning of a total of seventeen fixed markers with a Trimble R7 differential Global Positioning System (dGPS) unit. The interval between measurements varied between twenty-eight days for Biafo Glacier and six to twenty-two days for Baltoro Glacier (Quincey et al. 2009), although velocities are expressed in units of m per year^{-1} here for standardization. Permanent dGPS base stations do not exist in this region, so a temporary one was established in Skardu and run for the entire summer. We used the Precise Point Positioning technique and Trimble Geomatics Office software to process the dGPS data.

Velocities at the terminus of Biafo Glacier were 1.0 m per year^{-1} for a point located ~300 m from the terminus and 5.0 m per year^{-1} for a point located ~500 m from the terminus (Figure 10). These low values are characteristic for the lower parts of glaciers, although they also indicate that the glacier is active all the way to its terminus. This is further confirmed by Copland et al. (2009), who used feature tracking to determine velocities across the entire Biafo Glacier and found that velocities were low (<15 m year^{-1}) across most of the lower terminus but averaged 100 to 150 m per year^{-1} across most of the main ablation zone.

Surface velocities on Baltoro Glacier were generally much higher than Biafo, with a peak of ~240 m per year^{-1} recorded at two stakes at Gore II, ~12 km downglacier from Concordia (Quincey et al. 2009). Below this point the velocities gradually decreased over a distance of 23 km to a minimum of 10 m per year^{-1} at the glacier terminus. Velocities in the Concordia and K2 regions above Gore II varied between 125 and 168 m

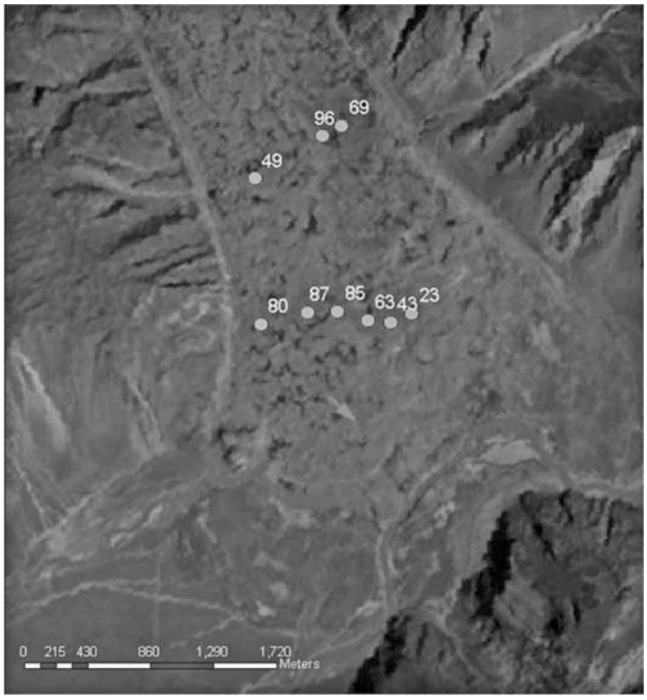

Figure 10. Ice depths in meters (green dots) and velocities in meters per year^{-1} (red arrows) measured across the terminus of Biafo Glacier in summer 2005.

Figure 11. View of the lowermost differential Global Positioning System measurement location on Baltoro Glacier (lower right foreground), with the tributary Uli Biaho Glacier visible in the background. Supraglacial debris thicknesses across the terminus of Baltoro Glacier are typically >1 m.

per year^{-1}. Comparisons with velocities derived from Synthetic Aperature Radar satellite imagery, feature tracking, and other field measurements (Mayer et al. 2006; Copland et al. 2009; Quincey et al. 2009) indicate generally good agreement for summer patterns but that the dGPS velocities are much higher than winter velocities over most of the glacier > 10 km upglacier from the terminus. These patterns suggest that motion of the lowermost ~10 km of the glacier is largely driven by ice deformation, whereas motion over the remainder of the ablation zone is dominated by basal sliding, with summer speed-ups of 200 percent or more compared to winter patterns (Quincey et al. 2009).

Surface Melt Rates

To sample a few surface melt rates, we placed ablation stakes at bare ice locations across Baltoro Glacier and remeasured them over periods of seven to nineteen days. The rates decreased with altitude, varying between 6.52 cm per day^{-1} at 3,907 m, 5.91 cm per day^{-1} at 4,055 m and 3.03 cm per day^{-1} at 4,837 m during a period with generally sunny weather and few clouds. These patterns agree well with those of Mihalcea et al. (2006), who also found a clear relationship between elevation and surface melt rates at Baltoro Glacier. Mihalcea et al. (2006) also found strong relationships between surface melt rates and surface debris thicknesses, with surface melt rates < 2.0 cm per day^{-1} when debris depths were > 0.10 m, regardless of elevation. Given the thick supraglacial debris cover over the lower part of Baltoro Glacier (Figure 11), it is likely that little melting occurs there.

The surface melt patterns provide an explanation for the observed velocity patterns, as the regions where the highest seasonal velocity variations occur are located at the lowest elevations where there is a bare ice surface. In these locations, large volumes of surface meltwater can make their way to the glacier bed via moulins and crevasses (Quincey et al. 2009) and produce high summer basal sliding rates. In contrast, the thick debris cover over the lowermost 10 km of the glacier occurs in a region where there is generally slow motion and a dominance of internal ice deformation. In this region the surface melt occurs only very slowly, producing little direct meltwater input to the glacier bed. The large volumes of meltwater from upglacier are presumably carried in hydraulically efficient subglacial channels that can remain open due to the low ice depths over the terminus.

Ice Depths

We measured ice depths with a monopulse ground-penetrating radar (GPR) system with a transmitter based on the design of Narod and Clarke (1994). The

receiver consisted of an airwave-triggered Tektronix digital oscilloscope connected to a handheld computer. We typically used a center frequency of 10 MHz, although in locations where the ice was particularly deep and the bed could not be seen at 10 MHz, we used 5 MHz. Errors in the ice-depth measurements are typically quoted as 1/10 of the transmitted wavelength (Bogorodsky, Bentley, and Gudmandsen 1985), which equates to ±1.7 m at 10 MHz and ±3.4 m at 5 MHz. The radiowave velocity of the GPR signals through the ice was assumed to be 0.168 m per ns^{-1}, an average value for temperate ice (Macheret, Moskalevsky, and Vasilenko 1993). We used a handheld Garmin eTrex GPS unit to locate the position of each GPR measurement to within ±10 m horizontally.

We measured ice depths at two profiles across Biafo Glacier, at distances of ~1 km and ~2 km from the ice front at surface elevations of ~3,200 m asl (Figure 10). The depths varied between 23 m and 85 m across the lower transect and 49 m and 96 m across the upper transect, in a part of the glacier that is heavily debris covered (average debris thickness ~1 m). The only other previous GPR measurements in this region were completed by Hewitt et al. (1989), who measured centerline ice depths of ~500 to 700 m at a transect ~25 km upglacier from the terminus (4,100 m asl) and depths up to ~1,400 m at the equilibrium line ~45 km upglacier from the terminus (4,650 m asl). These authors cautioned, however, that the measurements at the equilibrium line had a high degree of uncertainty.

On Baltoro Glacier, the greatest ice depth of 171 m occurred in proximity to the stakes with highest surface velocities at Gore II, with depths generally decreasing to a minimum of ~40 m at the glacier terminus (Figure 12). Ice was 141 to 155 m thick in the region of K2 base camp, although no successful measurements were made in the Concordia region. We suspect that the ice there was deeper, or perhaps the presence of more basal meltwater precluded our measurements with the GPR system, particularly because the ice is likely warm based. Desio, Marussi, and Caputo (1961) and Caputo (1964) reported measurements of ice depths on Baltoro Glacier that were determined using a gravimetric method in the mid-1950s for three locations:

1. At Urdukas, gravimetric ice depths were determined to be ~170 to 400 m, compared to depths up to 144 m in our study.
2. At Concordia, gravimetric ice depths were measured at up to ~850 m.

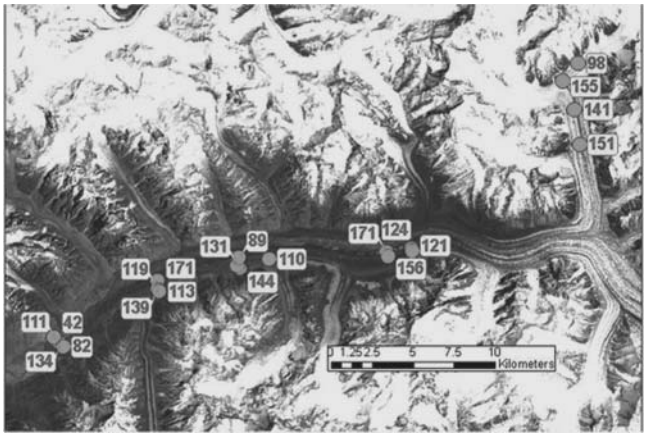

Figure 12. Ice depths (m) measured along Baltoro Glacier for summer 2005.

3. At K2 base camp, gravimetric ice depths were ~150 to 250 m, compared to 155 m in this study.

The gravimetric method exhibits a high degree of uncertainty and is therefore no longer used in glaciology, although the lower range of numbers just quoted are broadly comparable to the GPR measurements at Urdukas and K2 base camp. Given that the gravimetric method appears to have overestimated most depths, however, it is quite possible that ice depths at Concordia are lower than those quoted by Desio, Marussi, and Caputo (1961) and Caputo (1964). Based on repeat terrestrial photography of Concordia in 1912 and 2004, and the terminus of Baltoro Glacier in 1954 and 2004 (Mayer et al. 2006), there is little evidence that ice surface lowering has caused the differences in measured ice depths.

Discussion

Our climate simulations reveal a systematic pattern of increasing annual temperature and decreasing snow accumulation in the central Karakoram since the LGM. This result is consistent with long-term glacier retreat in the region (Mayewski and Jeschke 1979) and geomorphological evidence of extensive glaciations that generated high-altitude glacier erosion surfaces, U-shaped valleys exhibiting extreme relief, and extensive landslides that were most likely the result of debuttressing due to glacier retreat (Seong et al. 2007; Seong, Bishop et al. 2009). Furthermore, our paleoclimate simulations support our geochronology results of major glacier advances at ~16 and 11 ka, as snow accumulation was greater than modern-day conditions, and an enhanced monsoon in the Holocene would have

contributed much more summer snowfall compared to contemporary conditions.

Extensive glaciations during the Quaternary resulted in much greater ice depths than were measured in 2005, and our glacial reconstructions indicate that the ice was ~1 km thick in the Baltoro Valley near Biafo Glacier and much more extensive (Seong et al. 2007). Therefore, based on our current understanding of glacier erosion (ice depth and basal sliding velocity are the primary controls on abrasion), the magnitude of glacier erosion was much higher than contemporary erosion rates given more spatial coverage, thicker ice, and positive ice discharge. Furthermore, given the long-term retreat pattern caused by increasing temperatures and decreasing snow accumulation, glacier erosion during the retreat phases might have been greater than during advances, as increasing temperatures would produce more meltwater that governs basal water pressure, sliding velocity, and glacio-fluvial erosion. Koppes and Hallet (2006) indicated that there is a strong correlation between glacial retreat rates and glacial sediment yields.

Our geomorphometry results clearly indicate that relief is not linearly correlated with the HI in Pakistan. Although the K2 region of the central Karakoram exhibits the highest altitudes and high exhumation rates, it exhibits the lowest relief, yet the region has experienced significant erosion and exhumation (Foster, Gleadow, and Mortimer 1994; Seong et al. 2007, 2008). This apparent contradiction can be explained by nonlinear relationships between erosion and relief production.

Scale-dependent analysis revealed that in the absence of local high-discharge rivers and a spatially dense drainage network, variation in relief is dramatically reduced. As the K2 region of the central Karakoram has been dominated by glaciation and glacierization, glacier erosion can limit the relief at intermediate altitudes (Brozovic, Burbank, and Meigs 1997; Bishop, Shroder, and Colby 2003), thereby decreasing the variability in scale-dependent relief. Relatively low slope angles at intermediate altitudes document the erosion and redistribution of material by glaciers from 4,000 to 6,000 m asl. These low slope angles represent actual glacier surfaces or high-altitude erosion surfaces from past glaciations. These are classic signatures of a glacial buzzsaw. It is clear that the K2, Nanga Parbat, and Hunza regions have been significantly affected by glaciation, although the subsequent influence of local river incision and mass movement can increase local relief.

The highest scale-dependent relief occurs in the Hunza and Nanga Parbat regions and mesoscale relief patterns indicate that these regions are active erosion zones currently dominated by large-scale river incision and mass movement. The Hunza region exhibits more scale-dependent relief than Nanga Parbat because of an extensive fluvial drainage network. Our climate simulations suggest that the Hunza erosion zone, as depicted by mesoscale concave relief patterns, is the result of climate forcing. The region exhibits a negative snow accumulation anomaly in paleoclimate simulations that represent increased rainfall due to an intensification of the monsoon, where increased precipitation and associated river incision and mass movement explain the high scale-dependent relief. Furthermore, spatial patterns of precipitation have been found to be strongly controlled by topography in the Himalaya, and considerable variability exists at scales of ~10 km (Anders et al. 2006; Barros et al. 2006).

The K2 region of the central Karakoram is dominated by large glaciers and has less drainage network to produce additional local relief. This indicates that large-discharge rivers might not be required to focus erosion and produce uplift zones. At intermediate to higher altitudes, deep valley-glacier erosion and headwall erosion can effectively remove rock and sediment, whereas protective cold-based ice and permafrost on the highest peaks permits ridge and peak formation. Glacier mass-balance gradients determine the availability of meltwater for river incision and hillslope adjustment down-valley at lower altitudes. Consequently, in high mountain environments, glaciation both directly and indirectly alters the relief structure of the landscape differently with altitude. These differences can be attributed to the degree of temporal overprinting and spatial overlap of glacial events, such that at intermediate altitudes, the degree of spatial overlap is less than at high altitudes.

Therefore, with respect to glacier erosion and relief production, we should not expect relief to be related linearly to the magnitude of glacier erosion, as relief might not scale with erosional efficiency. Whipple (2009) indicated that erosional efficiency should be associated with a decrease in relief. Numerous parameters such as rock strength, topographic-induced stress fields, basal water pressures, basal sliding velocity, ablation rates related to climate and supraglacial debris loads, and other erosion processes determine the magnitude of glacier erosion, and isostatic and tectonic uplift operate at completely different spatio-temporal scales. Furthermore, glacier-erosion efficiency is most likely highly spatially variable in the Himalaya, as characterized by research on regional precipitation variability (e.g., Anders et al. 2006), our geomorphometric analysis, and mesoscale

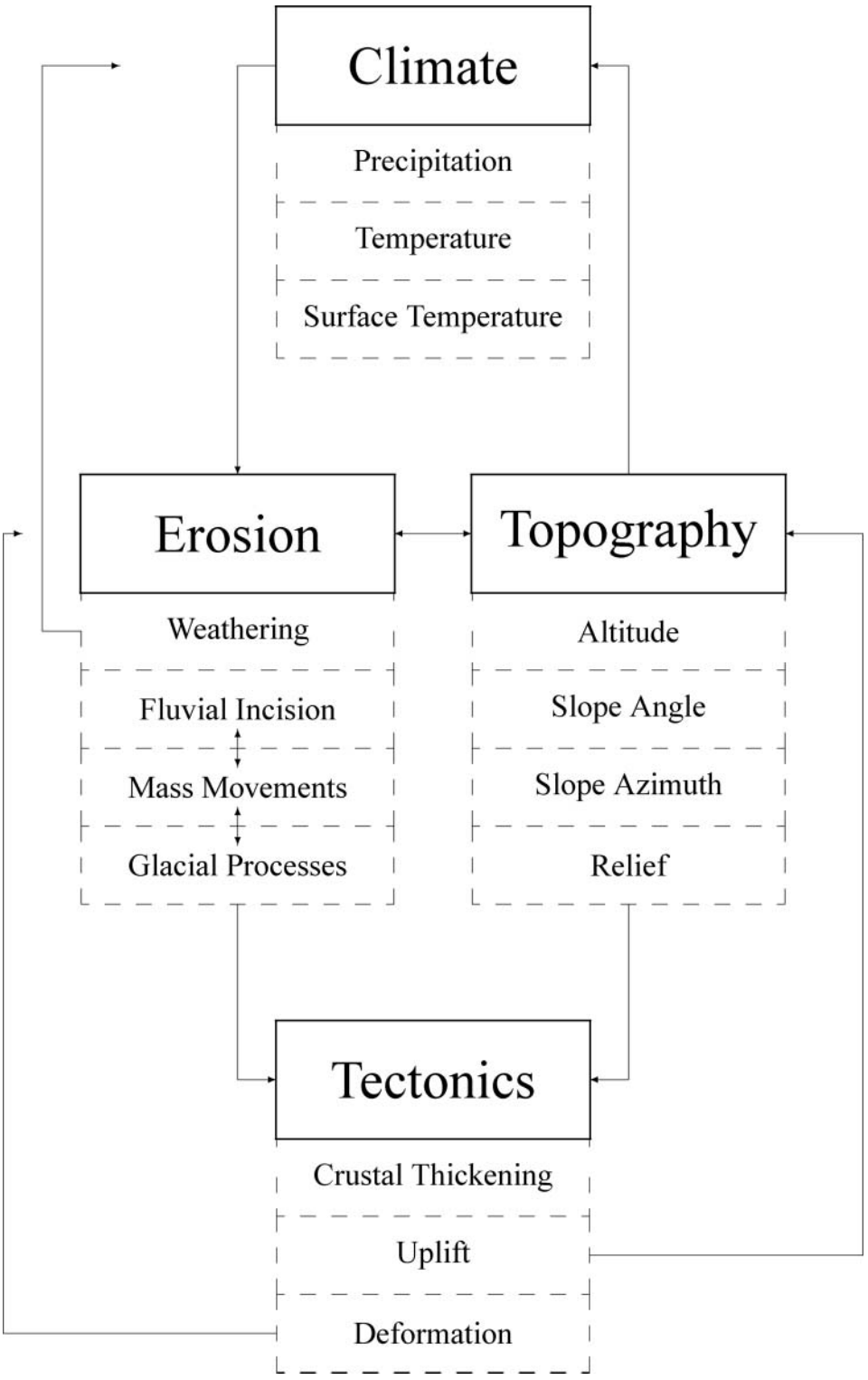

Figure 13. Interactions and selected feedback pathways for climate, erosion processes, and tectonics. Many parameters of the system are not included and the magnitudes of the linkages change with time. Positive and negative feedbacks exist for selected pathways.

relief variations that show little relief over the Kohistan region and Deosai plateau. Recent work by van der Beek et al. (2009) indicated that these two regions represent preserved remnants of the Eocene Tibetan plateau that have been glaciated and exhibit slow denudation. This demonstrates extreme spatio-temporal variability in the influence of glacier erosion in this region. Furthermore, large glaciers once flowed down all the major valleys in this region, significantly contributing to relief production. Such variability in climate change and erosion

patterns indicates that the landscape is unlikely to reach equilibrium in terms of mass or topographic steady state.

Modern-day glaciological conditions indicate that the glaciers are highly active and responding to climate forcing. The region is currently experiencing an increase in precipitation according to European reanalysis and Tropical Rainfall Measuring Mission data, and this appears to be associated with an increase in glacier surging and an expansion of nonsurging glaciers, as observed in satellite imagery. Furthermore, abundant meltwater and high glacier ice velocities indicate that glacier erosion potential might be increasing (Quincey et al. 2009).

Our more recent regional climate modeling simulations suggest that future increases in precipitation might be related to the strength of the westerly winds that are correlated with ENSO conditions. If this can be verified, these results would be in direct opposition to the hypothesis of an enhanced monsoon due to global warming (Anderson, Overpeck, and Gupta 2002). It is yet unclear whether an intensification of ENSO precipitation events or increases in atmospheric temperature will facilitate further glacier expansion or result in negative mass balance that will regulate the magnitude of glacier erosion. Our global climate simulation results suggest a future regional negative mass-balance trend.

Clearly, climate forcing has had a significant influence on landscape evolution in the western Himalaya of Pakistan. Large glaciers and glacier fluctuations have removed significant mass, thereby causing isostatic and tectonic uplift. The climate-versus-tectonic forcing hypotheses are difficult to relate directly, as numerous feedback mechanisms are involved, and direct linkages among climate, erosion, and tectonics must be established to demonstrate a tectonic response to climate change. Another important issue is whether active orogenic zones are carbon sinks or sources. Silicate weathering and the drawdown of atmospheric CO_2 could cause global cooling; however, climate simulations and radiative forcing explain glacier fluctuations in the Quaternary. Furthermore, chemical analyses of hot springs in the Himalaya suggest that active orogenic zones are sources of CO_2 caused by metamorphic reactions (Gaillardet and Galy 2008).

Climate forcing would intensify the geomorphic influence on crustal scale processes such that enhanced erosion causes the upward flow of hot, low-viscosity crustal rock into areas or localized uplift zones (Koons et al. 2002; Whipple 2009). Rapid erosion generates topographic stresses that reduce rock strength and intensify erosion in a positive feedback, thereby generating a strong crustal temperature and pressure gradient. Decompression melting and metamorphism is associated with rock flow along the gradient. Such erosional–rheological coupling can explain the presence of active metamorphic massifs (Koons et al. 2002). Metamorphic degassing of CO_2 would increase atmospheric concentrations. If this is the case, climate forcing and mountain building would inject CO_2 and warm Earth, resulting in limited glacier expansion and deglaciation. The hypothesis of orogenic CO_2 source contradicts the tectonic-forcing hypothesis and is dependent on the thermal history of the orogenic zone (Gaillardet and Galy 2008). Consequently, the climate-forcing hypothesis is predicated on whether mountain ranges are a net source or sink of atmospheric CO_2, and we must account for different processes and time scales such as the consumption of CO_2 by rock weathering (silicate and carbonate), the balance of organic matter burial and oxidation, and the fluxes of CO_2 degassing. It is also imperative that we better characterize the topography with respect to erosional efficiency and tectonic response so that the patterns of erosion and tectonics can be more directly related to climate forcing parameters.

Conclusions

Mountain geodynamics represent highly scale-dependent interactions involving climate, tectonic, and surface processes (Figure 13). The western Himalaya in Pakistan potentially exhibits strong climate–tectonic feedbacks, although the tectonic and topographic responses to climate perturbations have not been systematically explored. Nevertheless, the region exhibits unique patterns of topographic complexity, erosion, and exhumation.

Our GCM and regional-climate simulations suggest that the region has experienced extreme climate change due to radiative forcing and regional system response (i.e., westerlies, southwestern monsoon) to ENSO conditions. Paleoclimate simulations support geomorphological evidence of multiple glaciations and overall glacier retreat since the Holocene. High-magnitude glacier erosion has resulted in extreme relief, U-shaped valleys, high-altitude erosion surfaces, and extensive mass movements.

Our analysis of the topography indicates that relief is not related linearly to mass removal and erosional efficiency, as different surface processes and process couplings generate different topographic conditions that

vary with altitude and geologic structure. Consequently, in some locations the topography contains overprinting patterns regarding the polygenetic evolution of the landscape. This is not the case where high erosion and uplift rates generate threshold topography that might not sustain relief. Furthermore, mesocale relief patterns clearly depict erosion zones that are spatially coincident with precipitation anomalies, high peaks, and rapid exhumation. Mesoscale relief patterns demonstrate extreme spatial and temporal variability in the influence of glacier erosion in the topographic evolution of the region. Collectively, our results demonstrate a strong linkage between climate change and the topographic evolution of the central Karakoram in Pakistan. Nevertheless, Figure 13 clearly depicts that although climate and erosion play a significant role, the system is complex, with multiple feedback pathways and mechanisms operating at a multitude of spatio-temporal scales, such that the dominance of any particular component, process, or parameter of the system is likely to be highly variable and difficult to know with certainty. It is essential that we better characterize the topography with respect to erosional efficiency and tectonic response, so that the patterns of erosion and tectonics can be more directly related to climate forcing parameters.

Acknowledgments

We would especially like to acknowledge the long-term and highly fruitful relationship with the late Syed Hamidullah, former Director of the Centre of Excellence at Peshawar University, who worked so much to help facilitate this project. We would also like to thank his students, Faisal Khan and Mohammad Shahid, for their excellent assistance in the field. This research was supported by funding from the National Geographic Society and the U.S. National Science Foundation (Grant BCS-0242339) to the University of Nebraska–Omaha and the University of Cincinnati.

References

Anders, A. M., G. H. Roe, B. Hallet, D. R. Montgomery, N. J. Finnegan, and J. Putkonen. 2006. Spatial patterns of precipitation and topography in the Himalaya. In *Tectonics, climate, and landscape evolution*, ed. S. D. Willett, N. Hovius, M. T. Brandon, and D. M. Fisher, 39–53. Boulder, CO: Geological Society of America.

Anderson, D. M., J. T. Overpeck, and A. K. Gupta. 2002. Increase in the Asian southwest monsoon during the past four centuries. *Science* 297:596–99.

Barros, A. P., S. Chiao, T. J. Lang, D. Burbank, and J. Putkonen. 2006. From weather to climate: Seasonal and interannual variability of storms and implications for erosion processes in the Himalaya. In *Tectonics, climate, and landscape evolution*, ed. S. D. Willett, N. Hovius, M. T. Brandon, and D. M. Fisher, 17–38. Boulder, CO: Geological Society of America.

Beaumont, C., and G. Quinlan. 1994. A geodynamic framework for interpreting crustal-scale seismic-reflectivity patterns in compressional orogens. *Geophysics Journal International* 116:754–83.

Bender, F. K., and H. A. Raza. 1995. *Geology of Pakistan*. Berlin, Germany: Borntraeger.

Berger, A. 1992. Orbital variations and insolation database. IGBP PAGES/World Data Center-A for Paleoclimatology Data Contribution Series # 92–007, NOAA/NGDC Paleoclimatology Program, Boulder, CO.

Bishop, M. P., and J. F. Shroder, Jr. 2000. Remote sensing and geomorphometric assessment of topographic complexity and erosion dynamics in the Nanga Parbat massif. In *Tectonics of the Nanga Parbat syntaxis and the western Himalaya*, ed. M. Khan, P. J. Treloar, M. P. Searle, and M. Q. Jan, 181–200. London: Geological Society London.

———. 2004. *Geographic information science and mountain geomorphology*. Chichester, UK: Praxis-Springer.

Bishop, M. P., J. F. Shroder, Jr., R. Bonk, and J. Olsenholler. 2002. Geomorphic change in high mountains: A western Himalayan perspective. *Global and Planetary Change* 32:311–29.

Bishop, M. P., J. F. Shroder, Jr., and J. D. Colby. 2003. Remote sensing and geomorphometry for studying relief production in high mountains. *Geomorphology* 55:345–61.

Bogorodsky, V. V., C. R. Bentley, and P. E. Gudmandsen. 1985. *Radioglaciology*. Dordrecht, The Netherlands: Reidel.

Brozovic, N., D. W. Burbank, and A. J. Meigs. 1997. Climatic limits on landscape development in the northwestern Himalaya. *Science* 276:571–74.

Burbank, D. W., J. Leland, E. Fielding, R. S. Anderson, N. Brozovic, M. R. Reid, and C. Duncan. 1996. Bedrock incision, rock uplift and threshold hillslopes in the northwestern Himalayas. *Nature* 379:505–10.

Bush, A. B. G. 2001. Pacific sea surface temperature forcing dominates orbital forcing of the early Holocene monsoon. *Quaternary Research* 55:25–32.

———. 2007. Extratropical influences on the El Nino Southern Oscillation through the late Quaternary. *Journal of Climate* 20:788–800.

Bush, A. B. G., and S. G. H. Philander. 1999. The climate of the Last Glacial Maximum: Results from a coupled atmosphere–ocean general circulation model. *Journal of Geophysical Research* 104:509–25.

Caputo, M. 1964. Glaciology. In *Geophysics of the Karakorum*, ed. A. Marussi. Leiden, The Netherlands: E. J. Brill.

Cenderelli, D. A., and E. E. Wohl. 2003. Flow hydraulics and geomorphic effects of glacial-lake outburst floods in the Mount Everest region, Nepal. *Earth Surface Processes and Landforms* 28:385–407.

Christensen, J. H., J. Raisanen, T. Iversen, D. Bjorge, O. B. Christensen, and M. Rummukainen. 2001. A synthesis of regional climate change simulations: A Scandinavian perspective. *Geophysical Research Letters* 28:1003–6.

Clift, P. D., L. Giosan, J. Blusztajn, I. H. Campbell, C. Allen, M. Pringle, A. R. Tabrez, et al. 2008. Holocene erosion of the Lesser Himalaya triggered by intensified summer monsoon. *Geology* 36:79–82.

Clift, P. D., K. V. Hodges, D. Heslop, R. Hannigan, H. V. Long, and G. Calves. 2008. Correlation of Himalayan exhumation rates and Asian monsoon intensity. *Nature Geoscience* 1:875–80.

Copland, L., S. Pope, M. P. Bishop, J. F. Shroder, Jr., P. Clendon, A. B. G. Bush, U. Kamp, Y. B. Seong, and L. A. Owen. 2009. Glacier velocities across the central Karakoram. *Annals of Glaciology* 50:41–49.

Derbyshire, E. 1981. Glacier regime and glacial sediment facies: A hypothetical framework for the Qinghai-Xizang Plateau. In *Proceedings of the Symposium on Qinghai-Xizang (Tibet) Plateau,* vol. 2, 1649–56. Beijing: Science Press.

Desio, A., A. Marussi, and M. Caputo. 1961. Glaciological research of the Italian Karakorum Expedition 1953–1955. *IASH Publication* 52:224–32.

Easterling, D. R. 1999. Development of regional climate scenarios using a downscaling approach. *Climatic Change* 41:615–34.

Egholm, D. L., S. B. Nielsen, V. K. Pedersen, and J. E. Lesemann. 2009. Glacial effects limiting mountain height. *Nature* 460:884–88.

Finlayson, D. R., D. R. Montgomery, and B. Hallet. 2002. Spatial coincidence of rapid inferred erosion with young metamorphic massifs in the Himalayas. *Geology* 30:219–22.

Finnegan, N. J., B. Hallet, D. R. Montgomery, P. K. Zeitler, J. O. Stone, A. M. Anders, and L. Yuping. 2008. Coupling of rock uplift and river incision in the Namche Barwa–Gyala Peri massif, Tibet. *Geological Society of America Bulletin* 120:142–55.

Foster, D. A., A. J. W. Gleadow, and G. Mortimer. 1994. Rapid Pliocene exhumation in the Karakoram (Pakistan), revealed by fission-track thermochronology of the K2 gneiss. *Geology* 22:19–22.

Gaillardet, J., and A. Galy. 2008. Himalaya: Carbon sink or source? *Science* 320:1727–28.

Gerrad, A. J. 1990. *Mountain environments*. Cambridge, MA: MIT Press.

Gilchrist, A. R., M. A. Summerfield, and H. A. P. Cockburn. 1994. Landscape dissection, isostatic uplift, and the morphologic development of orogens. *Geology* 22:963–66.

Hagg, W., C. Mayer, A. Lambrecht, and A. Helm. 2008. Subdebris melt rates on Southern Inylchek Glacier, Central Tian Shan. *Geografiska Annaler Series A: Physical Geography* 90:55–63.

Hallet, B., L. Hunter, and J. Bogen. 1996. Rates of erosion and sediment evacuation by glaciers: A review of field data and their implications. *Global and Planetary Change* 12:213–35.

Hancock, G. S., R. S. Anderson, and K. X. Whipple. 1998. Beyond power: Bedrock river incision process and form. In *Rivers over rock: Fluvial processes in bedrock channels*, ed. K. J. Tinkler and E. E. Wohl, 35–60. Washington, DC: American Geophysical Union.

Harbor, J., and J. Warburton. 1992. Glaciation and denudation rates. *Nature* 356:751.

Hewitt, K. 1969. Glacier surges in the Karakoram Himalaya (Central Asia). *Canadian Journal of Earth Sciences* 6:1009–18.

———. 1988. Catastrophic landslide deposits in the Karakoram Himalaya. *Science* 242:64–77.

———. 1989. The altitudinal organisation of Karakoram geomorphic processes and depositional environments. *Zeitschrift für Geomorphologie* 76:9–32.

———. 1993. Altitudinal organization of Karakoram geomorphic processes and depositional environments. In *Himalaya to the sea,* ed. J. F. Shroder, Jr., 159–83. London and New York: Routledge.

———. 1998a. Catastrophic landslides and their effects on the Upper Indus streams, Karakoram Himalaya, northern Pakistan. *Geomorphology* 26:47–80.

———. 1998b. Glaciers receive a surge of attention in the Karakoram Himalaya. *Eos* 79:104–5.

———. 1999. Quaternary moraines vs. catastrophic avalanches in the Karakoram Himalaya, northern Pakistan. *Quaternary Research* 51:220–37.

———. 2005. The Karakoram anomaly? Glacier expansion and the "elevation effect," Karakoram Himalaya. *Mountain Research and Development* 25:332–40.

———. 2007. Tributary glacier surges: An exceptional concentration at Panmah Glacier, Karakoram Himalaya. *Journal of Glaciology* 53:181–88.

Hewitt, K., C. P. Wake, G. J. Young, and C. David. 1989. Hydrological investigations at Biafo Glacier, Karakorum Range, Himalaya: An important source of water for the Indus River. *Annals of Glaciology* 13: 103–8.

Howard, A. D. 1980. Thresholds in river regimes. In *Thresholds in geomorphology,* ed. D. R. Coates and J. D. Vitek, 227–58. London: Allen and Unwin.

Koons, P. O., P. K. Zeitler, C. P. Chamberlain, D. Craw, and A. S. Meltzer. 2002. Mechanical links between erosion and metamorphism in Nanga Parbat, Pakistan Himalaya. *American Journal of Science* 302:749–73.

Koppes, M., and B. Hallet. 2006. Erosion rates during rapid deglaciation in Icy Bay, Alaska. *Journal of Geophysical Research* 111:F02023.

Korup, O., and D. R. Montgomery. 2008. Tibetan plateau river incision inhibited by glacial stabilization of the Tsangpo gorge. *Nature* 455:786–90.

Macheret, Y. Y., M. Y. Moskalevsky, and E. V. Vasilenko. 1993. Velocity of radio waves in glaciers as an indicator of their hydrothermal state, structure and regime. *Journal of Glaciology* 39:373–84.

Mahéo, G., A. Pecher, S. Guillot, Y. Rolland, and C. Delacourt. 2004. Exhumation of Neogene gneiss domes between oblique crustal boundaries in south Karakorum (northwest Himalaya, Pakistan). In *Gneiss domes in orogeny,* ed. D. L. Whitney, C. Teyssier, and C. S. Siddoway, 141–54. Boulder, CO: Geological Society of America.

Mayer, C., A. Lambrecht, M. Belo, C. Smiraglia, and G. Diolaiuti. 2006. Glaciological characteristics of the ablation zone of Baltoro Glacier, Karakoram, Pakistan. *Annals of Glaciology* 43:123–31.

Mayewski, P. A., and P. A. Jeschke. 1979. Himalayan and Trans-Himalayan glacier fluctuations since AD 1812. *Arctic and Alpine Research* 11:267–87.

Mihalcea, C., C. Mayer, G. Diolaiuti, A. Lambrecht, C. Smiraglia, and G. Tartari. 2006. Ice ablation and meteorological conditions on the debris-covered area of Baltoro Glacier, Karakoram, Pakistan. *Annals of Glaciology* 43:292–300.

Minster, J. B., and T. H. Jordan. 1978. The present-day plate motions. *Journal of Geophysical Research* 83:5331–54.

Molnar, P. 1988. A review of the geophysical constraints on the deep structure of the Tibetan Plateau, the Himalaya and the Karakoram, and their tectonic implications. *Philosophical Transactions of the Royal Society of London, Series A* 326:33–88.

Molnar, P., and P. England. 1990. Late Cenozoic uplift of mountain ranges and global climatic change: Chicken or egg? *Nature* 46:29–34.

Montgomery, D. R. 1994. Valley incision and uplift of mountain peaks. *Journal of Geophysical Research* 99:913–21.

Montgomery, D. R., and M. T. Brandon. 2002. Topographic controls on erosion rates in tectonically active mountain ranges. *Earth and Planetary Science Letters* 201:481–89.

Narod, B. B., and G. K. C. Clarke. 1994. Miniature high-power impulse transmitter for radio-echo sounding. *Journal of Glaciology* 40:190–94.

Navarra, A., W. F. Stern, and K. Miyakoda. 1994. Reduction of the Gibbs oscillation in spectral model simulations. *Journal of Climatology* 7:1169–83.

Owen, L. A. 1988. Wet-sediment deformation of Quaternary and recent sediments in the Skardu Basin, Karakoram Mountains, Pakistan. In *Glaciotectonics: Forms and Processes*, ed. D. Croot, 123–48. Rotterdam, The Netherlands: Balkema.

Owen, L. A., M. W. Caffee, K. Bovard, R. C. Finkel, and M. Sharma. 2006. Terrestrial cosmogenic surface exposure dating of the oldest glacial successions in the Himalayan orogen. *Geological Society of America Bulletin* 118: 383–92.

Owen, L. A., M. W. Caffee, R. C. Finkel, and Y. B. Seong. 2008. Quaternary glaciations of the Himalayan-Tibetan orogen. *Journal of Quaternary Science* 23:513–32.

Owen, L. A., R. C. Finkel, P. L. Barnard, M. Haizhhou, K. Asahi, M. W. Caffee, and E. Derbyshire. 2005. Climatic and topographic controls on the style and timing of Late Quaternary glaciations throughout Tibet and the Himalaya defined by ^{10}Be cosmogenic radionuclide surface exposure dating. *Quaternary Science Reviews* 24:1391–1411.

Owen, L. A., R. C. Finkel, M. W. Caffee, and L. Gualtieri. 2002. Timing of multiple glaciations during the Late Quaternary in the Hunza Valley, Karakoram Mountains, Northern Pakistan: Defined by cosmogenic radionuclide dating of moraines. *Geological Society of America Bulletin* 114:593–604.

Owen, L. A., L. Gualtieri, R. C. Finkel, M. W. Caffee, D. I. Benn, and M. C. Sharma. 2001. Cosmogenic radionuclide dating of glacial landforms in the Lahul Himalaya, Northern India: Defining the timing of Late Quaternary glaciation. *Journal of Quaternary Science* 16:555–63.

Pant, G. B., and K. R. Kumar. 1997. *Climates of South Asia*. Chichester, UK: Wiley.

Pelletier, J. D. 2008. Glacial erosion and mountain building. *Geology* 36:591–92.

Peltier, W. R. 1994. Ice age paleotopography. *Science* 265:195–201.

Pratt-Sitaula, B., B. N. Upreti, T. Melbourne, A. Miner, E. Parker, S. M. Rai, and T. N. Bhattarai. 2009. Applying geodesy and modeling to test the role of climate controlled erosion in shaping Himalayan morphology and evolution. *Himalayan Geology* 30:123–31.

Quincey, D. J., L. Copland, C. Mayer, M. P. Bishop, A. Luckman, and M. Belo. 2009. Ice velocity and climate variations for the Baltoro Glacier, Pakistan. *Journal of Glaciology* 55:1061–71.

Rahaman, W., S. K. Singh, R. Sinha, and S. K. Tandon. 2009. Climate control on erosion distribution over the Himalaya during the past ~100 ka. *Geology* 37:559–62.

Raisanen, J., M. Rummukainen, and A. Ullerstig. 2001. Downscaling of greenhouse gas induced climate change in two GCMs with the Rossby Centre regional climate model for northern Europe. *Tellus Series A* 53:168–91.

Raymo, M. E., and W. F. Ruddiman. 1992. Tectonic forcing of late Cenozoic climate. *Nature* 359:117–22.

Raymo, M. E., W. F. Ruddiman, and P. N. Froelich. 1988. Influence of late Cenozoic mountain building on ocean geochemical cycles. *Geology* 16:649–53.

Schmidt, K. M., and D. R. Montgomery. 1995. Limits to relief. *Science* 270:617–20.

Schoof, J. T., and S. C. Pryor. 2001. Downscaling temperature and precipitation: A comparison of regression-based methods and artificial neural networks. *International Journal of Climatology* 21:773–90.

Searle, M. P. 1991. *Geology and tectonics of the Karakoram Mountains*. Chichester, UK: Wiley.

Searle, M. P., R. R. Parrish, R. Tirrul, and D. C. Rex. 1990. Age of crystallization and cooling of the K2 gneiss in the Baltoro Karakoram. *Journal of the Geological Society of London* 147:603–6.

Seong, Y. B., M. P. Bishop, A. B. G. Bush, P. Clendon, L. Copland, R. C. Finkel, U. Kamp, L. A. Owen, and J. F. Shroder, Jr. 2009. Landforms and landscape evolution in the Skardu, Shigar and Braldu Valleys, Central Karakoram. *Geomorphology* 103:251–67.

Seong, Y. B., L. A. Owen, M. P. Bishop, A. B. G. Bush, P. Clendon, L. Copland, R. C. Finkel, U. Kamp, and J. F. Shroder, Jr. 2007. Quaternary glacial history of the Central Karakoram. *Quaternary Science Reviews* 26:3384–405.

———. 2008. Rates of fluvial bedrock incision within an actively uplifting orogen: Central Karakoram Mountains, northern Pakistan. *Geomorphology* 97:274–86.

Seong, Y. B., L. A. Owen, C. Yi, R. C. Finkel, and L. Schoenbohm. 2009. Geomorphology of anomalously high glaciated mountains at the northwestern end of Tibet: Muztag Ata and Kongur Shan. *Geomorphology* 103:227–50.

Shi, Y. 2002. Characteristics of late Quaternary monsoonal glaciation on the Tibetan Plateau and in East Asia. *Quaternary International* 97–98:79–91.

Shroder, J. F., Jr. 1998. Slope failure and denudation in the western Himalaya. *Geomorphology* 26:81–105.

Shroder, J. F., Jr., and M. P. Bishop. 2000. Unroofing of the Nanga Parbat Himalaya. In *Tectonics of the Nanga Parbat syntaxis and the western Himalaya*, ed. M. Khan, P. J.

Treloar, M. P. Searle, and M. Q. Jan, 163–79. London: Geological Society of London.

Sklar, L. S., and W. E. Dietrich. 1998. River longitudinal profiles and bedrock incision models: Stream power and the influence of sediment supply. In *Rivers over rock: Fluvial processes in bedrock channels*, ed. K. J. Tinkler and E. E. Wohl, 237–60. Washington, DC: American Geophysical Union.

———. 2001. Sediment and rock strength controls on river incision into bedrock. *Geology* 29:1087–90.

Spotila, J. A., J. T. Buscher, A. J. Meigs, and P. W. Reiners. 2004. Long-term glacial erosion of active mountain belts: Example of the Chugach-St. Elias Range, Alaska. *Geology* 32:501–04.

Tomkin, J. H., and J. Braun. 2002. The influence of alpine glaciations on the relief of tectonically active mountain belts. *American Journal of Science* 302:169–90.

Turcotte, D. L., and G. Schubert. 2002. *Geodynamics*. Cambridge, UK: Cambridge University Press.

van der Beek, P., J. Van Melle, S. Guillot, A. Pecher, P. W. Reiners, S. Nicolescu, and M. Latif. 2009. Eocene Tibetan plateau remnants preserved in the northwest Himalaya. *Nature Geoscience* 2:364–68.

von Storch, H., and A. Navarra. 1999. *Analysis of climate variability*. New York: Springer.

Wake, C. P. 1989. Glaciochemical investigations as a tool for determining the spatial and seasonal variation of snow accumulation in the central Karakoram, northern Pakistan. *Annals of Glaciology* 13:279–84.

Whipple, K. X. 2009. The influence of climate on the tectonic evolution of mountain belts. *Nature Geoscience* 2:97–104.

Whipple, K. X., E. Kirby, and S. H. Brocklehurst. 1999. Geomorphic limits to climate-induced increases in topographic relief. *Nature* 401:39–43.

Whipple, K. X., and G. E. Tucker. 1999. Dynamics of the stream-power river incision model: Implications for height limits of mountain ranges, landscape response timescales, and research needs. *Journal of Geophysical Research* 104:17661–74.

Whittington, A. G. 1996. Exhumation overrated. *Tectonophysics* 206:215–26.

Wobus, C., K. X. Whipple, E. Kirby, N. Snyder, J. Johnson, K. Spyropolou, B. Crosby, and D. Sheehan. 2006. Tectonics from topography: Procedures, promise and pitfalls. In *Tectonics, climate, and landscape evolution*, ed. S. D. Willett, N. Hovius, M. T. Brandon, and D. M. Fisher, 55–74. Boulder, CO: Geological Society of America.

Wohl, E. 2000. Mountain rivers. Water Resources Monograph 14, American Geophysical Union, Washington, DC.

Yokoyama, R., M. Shirasawa, and R. J. Pike. 2002. Visualizing topography by openness: A new application of image processing to digital elevation models. *Photogrammetric Engineering and Remote Sensing* 68:257–65.

Zeitler, P. K. 1985. Cooling history of the NW Himalaya. *Tectonics* 4:127–51.

Zeitler, P. K., P. O. Koons, M. P. Bishop, C. P. Chamberlain, D. Craw, M. A. Edwards, S. Hamidullah, et al. 2001. Crustal reworking at Nanga Parbat, Pakistan: Metamorphic consequences of thermal-mechanical coupling facilitated by erosion. *Tectonics* 20:712–28.

Zeitler, P. K., A. S. Meltzer, P. O. Koons, D. Craw, B. Hallet, C. P. Chamberlain, W. S. F. Kidd, et al. 2001. Erosion, Himalayan geodynamics and the geomorphology of metamorphism. *Geological Society of America Today* 11:4–8.

Correspondence: Department of Geography and Geology, University of Nebraska–Omaha, Omaha, NE 68182-0199, e-mail: mpbishop@mail.unomaha.edu (Bishop); jshroder@mail.unomaha.edu (Shroder); Department of Earth and Atmospheric Sciences, University of Alberta, Edmonton, Alberta T6G 2E3, Canada, e-mail: andrew.bush@ualberta.ca (Bush); Department of Geography, University of Ottawa, Ottawa, Ontario K1N 6N5, Canada, e-mail: luke.copland@uottawa.ca (Copland); Department of Geography, The University of Montana, Missoula, MT 59812-5040, e-mail: ulrich.kamp@umontana.edu (Kamp); Department of Geology, University of Cincinnati, Cincinnati, OH 45221-0013, e-mail: lewis.owen@uc.edu (Owen); Department of Earth and Environmental Sciences, Korea University, Seoul, 136–704, Korea, e-mail: ybseong@hotmail.com (Seong).